



UNIVERSITY OF LEEDS

This is a repository copy of *Mitigation of state of charge estimation error due to noisy current input measurement*.

White Rose Research Online URL for this paper:

<https://eprints.whiterose.ac.uk/201359/>

Version: Published Version

Article:

Kadem, O. orcid.org/0000-0002-4192-1047 and Kim, J. orcid.org/0000-0002-3456-6614
(2023) Mitigation of state of charge estimation error due to noisy current input measurement. Proceedings of the Institution of Mechanical Engineers, Part I: Journal of Systems and Control Engineering. ISSN 0959-6518

<https://doi.org/10.1177/09596518231182308>

Reuse

This article is distributed under the terms of the Creative Commons Attribution (CC BY) licence. This licence allows you to distribute, remix, tweak, and build upon the work, even commercially, as long as you credit the authors for the original work. More information and the full terms of the licence here:

<https://creativecommons.org/licenses/>

Takedown

If you consider content in White Rose Research Online to be in breach of UK law, please notify us by emailing eprints@whiterose.ac.uk including the URL of the record and the reason for the withdrawal request.



eprints@whiterose.ac.uk
<https://eprints.whiterose.ac.uk/>

Mitigation of state of charge estimation error due to noisy current input measurement

Onur Kadem  and Jongrae Kim

Proc IMechE Part I:
J Systems and Control Engineering
1–13

© IMechE 2023



Article reuse guidelines:

sagepub.com/journals-permissions

DOI: 10.1177/09596518231182308

journals.sagepub.com/home/pii



Abstract

The key indicator to assess the performance of a battery management system is the state of charge (SoC). Although various SoC estimation algorithms have been developed to increase the estimation accuracy, the effect of the current input measurement error on the SoC estimation has not been adequately considered in these algorithms. The majority of SoC estimation algorithms are based on noiseless current measurement models in the literature. More realistic battery models must include the current measurement modelled with the bias noise and the white noise. We present a novel method for mitigating noise in current input measurements to reduce the SoC estimation error. The proposed algorithm is validated by computer simulations and battery experiments. The results show that the proposed method reduces the maximum SoC estimation error from around 11.3% to 0.56% in computer simulations and it is reduced from 1.74% to 1.17% in the battery experiment.

Keywords

State of charge estimation error, noisy current input measurement, online parameter estimation, adaptive Kalman filtering, current noise mitigation

Date received: 11 December 2022; accepted: 19 April 2023

Introduction

Concerns regarding energy conservation and environmental protection have increased the popularity of electric vehicles (EVs). Despite their increasing popularity, their performance still need to be improved. Existing EVs have a significantly lower driving range compared to traditional internal combustion engine-based vehicles. Another issue regarding EVs is to miscalculate the remaining power, leaving passengers stranded. These are due to the lack of an efficient battery management system (BMS) that can accurately estimate the remaining power of a battery pack. In this sense, the state of charge (SoC) is a key parameter to ensure a longer driving range with reliable remaining power. Optimal SoC estimation maximises battery energy utilisation, resulting in increased driving range. It is also vital to inform the driver about the current driving range and avoid the harmful consequences of overcharging or over-discharging the battery. The majority of investigations to improve the SoC estimation accuracy primarily focus on algorithm development with no current measurement error assumption.

The SoC is the ratio of the available battery capacity to the maximum battery capacity.¹ It cannot be directly measured but can be calculated or estimated using current and voltage measurements. There are various types of SoC estimation algorithms divided into two main groups: model-free methods and model-based methods.² Two most widely used model-free methods are Coulomb counting (CC) and open circuit voltage (OCV) measurement methods. The CC method determines the remaining capacity of a battery by integrating the current flowing in and out of the battery over time. However, noisy current measurement is not the only disadvantage of this method but also the correct initial SoC guess is required for high accuracy.³ The OCV measurement method measures the terminal

Institute of Design, Robotics, & Optimisation (iDRO), School of Mechanical Engineering, University of Leeds, Leeds, UK

Corresponding author:

Onur Kadem, Institute of Design, Robotics, & Optimisation (iDRO), School of Mechanical Engineering, University of Leeds, Leeds LS2 9JT, UK.
Email: mn16ok@leeds.ac.uk

voltage when the battery is in a steady state for a sufficient time, for example, 1 h.⁴ The measured terminal voltage is assumed to be equal to the OCV and then converted to the SoC through a look-up table, which is obtained by laborious laboratory work. This method is not practical since it requires a long relaxation period and a look-up table.

State of health (SoH) is another important indicator in battery systems and it refers to how well a battery is performing in comparison to its fresh condition. In literature, there are various approaches to calculating SoH accurately. In the work by Guo et al.,⁵ an SoH estimation algorithm using the SSA-Elman model is proposed. Battery features and capacity are better correlated using this method. In the work by Li et al.,⁶ an improved electrochemical impedance spectroscopy (EIS) method is introduced to estimate SoH. The improved method increases the equivalent circuit model (ECM) accuracy and reduces the error in the SoH estimation error. An attention mechanism and bidirectional long short-term memory neural network are combined in Guo et al.⁷ for estimating SoH. Three features as input of the model are chosen from the incremental capacity curve.

Model-based SoC estimation algorithms require a battery model to reflect the battery dynamics. Electrochemical models and ECMs are the two most common techniques used in battery modelling. In electrochemical models, complex differential equations are used to describe the electrochemical process taking place inside the battery.⁸ The pseudo-two-dimensional (P2D) model is one of the electrochemical models existing in the literature. P2D models are based on the porous electrode theory, concentrated solution theory and kinetic equations.⁹ Another electrochemical model is the single-particle model (SPM) which was developed to simplify the P2D model. In the SPM, it is assumed that multiple uniform-sized spherical particles form the electrodes and the current distribution is uniform along both electrodes.¹⁰ The electrochemical models can explain battery dynamics in terms of the main electrochemical reactions occurring inside a battery. However, their onsite accuracy is low due to their complexity and numerous parameters to be identified in the models. They are generally used for the optimisation of the battery design.¹¹ Unlike the electrochemical models, the ECMs are frequently used in estimating the SoC due to the advantages of low computational effort and high estimation accuracy. The ECM describes the battery dynamics via basic circuit elements. In the work by Feng et al.¹² and Hossain et al.,¹³ it is shown that the Thevenin ECM model with one parallel resistor-capacitor (RC) branch can accurately represent the battery dynamics.

Adopting a battery model requires model parameter identification (MPI). The MPI methods are classified into two main groups: an offline method and online methods. The offline method is an experimental method to calculate the model parameters in

laboratories. The hybrid pulse power characterisation (HPPC) current profile is commonly used in the experiment.¹⁴ This method provides fixed parameter estimations. The actual model parameters change as the battery ages and the operational conditions change. Therefore, offline method cannot update the parameters according to different operational conditions and battery ageing, resulting in inaccurate SoC estimates. To adopt the parameters to the changes in operational conditions and battery ageing, online MPI methods are used. The recursive least squares (RLS) method is one of the most popular online methods found in literature.^{15,16} In the work by Xia et al.,¹⁷ a forgetting factor RLS method is introduced to minimise the influence of old data on the current estimate. However, the noisy current input measurement deteriorates the performance of RLS-based parameter identification methods.¹⁸ In this case, the adaptive law-based MPI method can be an alternative. This method guarantees the stability of the parametric uncertainties based on the Lyapunov direct method.¹⁹

The Kalman filter (KF) family has been used in ECM-based SoC estimation algorithms due to its simplicity and powerful estimation ability.^{20–23} These algorithms first estimate the OCV and then convert it to the SoC using the nonlinear relationship between the SoC and the OCV.^{24,25} In the literature, the majority of available SoC estimation algorithms do not consider the input current measurement noise. The development of a more realistic SoC estimation algorithm requires taking into account the input noise.

Error is always present in the current measurement, which is the input of both current counting and voltage-based correction methods. Thus, the current measurement error causes SoC error in both methods.²⁶ The current measurement is corrupted by the current bias noise and the white noise.^{27,26} The impact of these noises is significantly different. The white noise does not have a significant effect on the SoC estimation error.²⁸ The extended Kalman filter (EKF) can accurately estimate the SoC based on the current sensor measurement with the large random white noise.²⁹ However, it is found that the bias noise substantially increases the error in the SoC estimation.²⁷ In the work by Liu and He,³⁰ the effect of the bias noise on the SoC estimation is investigated. The bias noise of ± 10 A is injected into the SoC estimation algorithm during the simulation. It is observed that the SoC estimation error is out of the tolerable range by 5%, which may cause overcharging or discharging of the battery in real-time applications. In the work by Liu et al.,³¹ it is found that the bias noise may reach up to 1% in the battery experiments. It can reach up to 200 mA in practice due to the electromagnetic environment and the temperature. In the work by Liu et al.,³¹ the bias noise is treated as a constant parameter to be estimated with battery model parameters. The convergence of battery model parameters to their actual values is not guaranteed; therefore, the bias convergence to its actual value

cannot be guaranteed. Incorrect bias estimation would lead to erroneous SoC estimation. In the work by Xu et al.,²¹ a dual KF algorithm is proposed to filter the SoC twice to reduce the current measurement error and battery modelling error. Despite the increased computational cost, this method cannot provide a certain mitigation of the bias noise. In the work by Hou et al.,³² the SoC is estimated for portable devices without sensing the current. The current is an unknown input that is chosen as one of the states. In the work by Chun et al.,³³ a method is also developed to estimate the SoC without sensing the current measurement. The method only uses the filtered terminal voltage measurements of each cell in the battery pack. The current applied to the battery is estimated using the corresponding filtered terminal voltage measurement. To estimate the load current based on terminal voltage sensor measurements, it is necessary to use a high-quality but costly voltage sensor; otherwise, the current estimate is likely to be less accurate. An improved fuzzy adaptive KF is designed in Yan et al.³⁴ to estimate the SoC of EVs working under poor sensor measurements. The system noise and the measurement noise are assumed to be zero-mean white noise, and the proposed method only updates their statistical properties. However, the current sensor is also corrupted by the bias noise and it is neglected.

In literature, different noise modelling strategies have been considered. In the work by Wang et al.,³⁵ a method is proposed to calculate the error probabilities, which characterises the estimation reliability and diagnosis accuracy stochastically. To investigate sensor measurements, data missing phenomenon is considered to address the estimation error in Chen et al.³⁶ In the work by Kitaniadis,³⁷ the uncertainty in the system input is modelled as a stochastic process with a mean value that is not known and varies in time. In the work by Shu et al.,³⁸ the corrupted measurements are characterised as a Bernoulli-distributed random sequence. In the work by Lu et al.,³⁹ it is shown that the states and unknown system inputs can be estimated by an extended Double-Model adaptive estimation approach. The unknown time-varying input is modelled as a random walk. Then, the system and measurement models are updated based on the unknown input model. Finally, the estimation algorithm is updated based on the new system and measurement models. In this work, we modelled the current sensor as a summation of the true current, the bias noise treated as random walk and the zero-mean white noise. To the best of the authors' knowledge, our work is the first direct attempt to consider two stochastic noises in the current measurement in the SoC estimation.

The organisation of the article is as follows: section 'Adaptive battery model identification' introduces the battery modelling and online MPI method, section 'Current bias mitigation' explains the bias noise estimation method; section 'SoC estimation' presents the SoC estimation method along with the modification of the

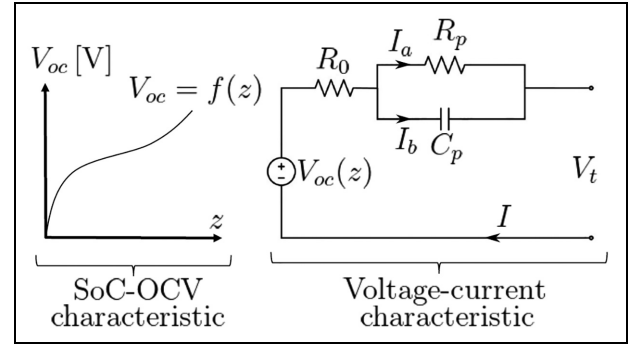


Figure 1. SoC–OCV nonlinear relationship and equivalent circuit model of Li-ion battery.

standard KF algorithm; section 'Simulations and results' presents the computer simulation and experimental results; finally, the conclusion and the future work are presented in section 'Conclusion and future work'.

Adaptive battery model identification

Equivalent circuit battery modelling

An accurate SoC estimation algorithm can be developed based on a battery model, which is required for the safe and efficient operation of the battery. The ECM-based battery models have been used to replicate the battery dynamic behaviour.⁴⁰ There are several ECMs found in the literature. Although Thevenin-based ECMs do not demand comprehensive knowledge regarding battery electrochemistry, they accurately reflect the battery dynamics.^{41,42} The first-order Thevenin model is revealing superiority over other ECMs due to its simplicity but accuracy in representing the battery dynamics.^{43–45,46} Figure 1 shows the ECM used in this work. The ECM has an ideal OCV source (V_{oc}), an ohmic resistance (R_0) and an RC branch consisting of a polarisation resistor R_p and a polarisation capacitor C_p . The energy loss during charging or discharging the battery is caused by R_0 . The RC branch mimics the polarisation characteristic of the battery during or after the charging/discharging cycles. The load current and the terminal voltage signals are denoted by I and V_t , respectively. I_a is the current flowing over R_p , whereas I_b is the current flowing over C_p . The battery reaches the equilibrium state in a sufficient enough time, for example, 1 h after the load is removed from the battery. In the equilibrium state, V_t is equal to V_{oc} . Herein, the load current has a positive sign at discharge and a negative sign at charge. Based on the Kirchhoff's law and Ohm's law, the first-order Thevenin ECM can be expressed as follows

$$\frac{dV_p}{dt} = \frac{I}{C_p} - \frac{V_p}{R_p C_p} \quad (1a)$$

$$V_t = V_{oc} - IR_0 - V_p \quad (1b)$$

where t is the time, d/dt is the derivative, V_p is the voltage across the RC branch. In equation (1), R_0 , R_p and C_p are the model parameters to be identified. Furthermore, the identification of the nonlinear SoC–OCV relationship is also necessary for the SoC estimation. This relationship can be acquired through a battery SoC drop test.

Online MPI

An online MPI method improves the real-time performance of SoC estimation algorithms. In this work, the adaptive law-based MPI method is adopted to estimate the model parameters in real time. The adaptive law calculates the current estimate of the parameters by adding the previous estimate of the parameters and the correction term. The correction term is calculated based on a difference between the calculated output signal and the measured output signal. Therefore, the model parameter uncertainty is overcome by parameter updating and correction.

Discrete-time expressions of equations (1a) and (1b) are of the form

$$V_{p,k+1} = \alpha V_{p,k} + (1 - \alpha)R_p I_k \quad (2a)$$

$$V_{t,k} = V_{oc,k} - R_0 I_k - V_{p,k} \quad (2b)$$

where $(\cdot)_k$ represents the k th sample of (\cdot) , $\alpha = e^{-\Delta t/\tau}$, Δt is the sampling time and τ is the time constant, that is, $\tau = R_p C_p$. Rewrite equation (2b) for step $k + 1$

$$V_{t,k+1} = V_{oc,k+1} - R_0 I_{k+1} - V_{p,k+1} \quad (3)$$

Substitute equation (2a) into equation (3)

$$V_{t,k+1} = V_{oc,k+1} - R_0 I_{k+1} - \alpha V_{p,k} - (1 - \alpha)R_p I_k \quad (4)$$

Rearrange equation (2b) and substitute into equation (4)

$$V_{t,k+1} = \alpha V_{t,k} - R_0 I_{k+1} + [\alpha R_0 - (1 - \alpha)R_p] I_k + V_{oc,k+1} - \alpha V_{oc,k} \quad (5)$$

Define $\Delta V_{t,k+1} = V_{t,k+1} - V_{t,k}$ and substitute into equation (5) for sampling time k and $k - 1$

$$\Delta V_{t,k+1} = \alpha \Delta V_{t,k} - R_0 \Delta I_{k+1} + \gamma \Delta I_k + \Delta V_{oc,k+1} - \alpha \Delta V_{oc,k} \quad (6)$$

where $\Delta(\cdot)_{k+1} = (\cdot)_{k+1} - (\cdot)_k$ and $\gamma = \alpha R_0 - (1 - \alpha)R_p$. V_{oc} varies slowly in comparison with V_t , when the

sampling frequency is high enough,⁴⁷ that is, $\Delta V_{oc} \approx 0$. Equation (6) can be approximated as follows

$$\Delta V_{t,k+1} = \alpha \Delta V_{t,k} - R_0 \Delta I_{k+1} + \gamma \Delta I_k \quad (7)$$

Equation (7) can be written in the LPM as follows

$$y_{k+1} = \theta_{k+1}^T \phi_{k+1} \quad (8)$$

where the unknown model parameters vector is given by

$$\theta_{k+1} = [\alpha \quad -R_0 \quad \gamma]^T \quad (9)$$

and the measured input vector is given by

$$\phi_{k+1} = [\Delta V_{t,k} \quad \Delta I_{k+1} \quad \Delta I_k]^T \quad (10)$$

The terminal voltage difference is calculated from two measurement samples. The measurement equation for the parameter estimation is as follows

$$\tilde{y}_{k+1} = \Delta V_{t,k+1} + \Delta v_{V_t,k+1} \quad (11)$$

where $(\tilde{\cdot})$ is the measurement of (\cdot) and $\Delta v_{V_t,k+1}$ represents the measurement noise. Note that unadorned symbols represent the true values.

θ_k is simultaneously estimated using the online parameter estimation method based on the adaptive law given as follows⁴⁸

$$\varepsilon_{k+1} = \tilde{y}_{k+1} - \hat{\theta}_k^T \phi_{k+1} \quad (12a)$$

$$\hat{\theta}_{k+1} = \hat{\theta}_k + \Gamma \Delta t \varepsilon_{k+1} \phi_{k+1} \quad (12b)$$

where $(\hat{\cdot})$ is the estimate of (\cdot) , and Γ is the positive-definite adaptive gain matrix. After $\hat{\theta}_k$ is calculated, the model parameters \hat{R}_0 , \hat{R}_p and \hat{C}_p can be reversely calculated by

$$\hat{R}_0 = -\hat{\theta}_{k+1}^{(2)} \quad (13a)$$

$$\hat{R}_p = \frac{\hat{\theta}_{k+1}^{(3)} + \hat{\theta}_{k+1}^{(1)} \hat{R}_0}{1 - \hat{\theta}_{k+1}^{(1)}} \quad (13b)$$

$$\hat{C}_p = \frac{-\Delta t \hat{R}_p}{\log \hat{\theta}_{k+1}^{(1)}} \quad (13c)$$

where $(\cdot)^{(i)}$ for $i = 1, 2, 3$ is the i th element of (\cdot) .

Test rig design

Figure 2 shows a schematic diagram of the test rig designed to run three DC motors powered by a completely new lithium polymer (LiPo) battery whose

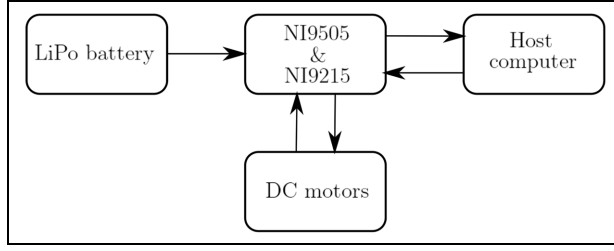


Figure 2. The schematic diagram of experimental setup.

Table 1. The operational conditions in the experiment.

Battery condition	Fresh battery
Operating temperature	25°C ± 3°C
Upper cut-off voltage	8.4 V
Lower cut-off voltage	6.4 V
Discharge current	1.3 A

capacity is 1 Ah. The battery has two serially connected LiPo cells, which makes the battery's upper cut-off voltage 8.4 V and lower cut-off voltage 6.4 V. CompactRIO is the microprocessor used in the test rig. A graphical user interface is designed on LabVIEW software to control the speed of DC motors. During the battery test, I and V_t are measured through the NI 9505 and NI 9215 devices every 0.01 s. We used a commercial battery charger to charge the battery in a constant current constant voltage (CCCV) mode. It can also be used to discharge the battery with a constant current. To prevent possible electrode damage due to overcharging the battery, the upper cut-off voltage is set to 8.4 V. When the terminal voltage drops to 6.4 V, the battery is considered completely discharged. The operating temperature remains constant at 25°C ± 3°C. Three DC motors discharge the battery with a constant current of 1.3 A when the speed is set to 50 r/min (revolution per minute). The speed remains constant at 50 r/min during the battery experiment. The experimental conditions are summarised in Table 1.

SoC–OCV nonlinear relationship

All ECM-based SoC estimation algorithms require the nonlinear SoC–OCV relationship to convert the estimated OCV to an SoC estimate. This relationship can be obtained by a battery SoC drop test.⁴⁹ First, the battery is fully charged under a CCCV regime until it reaches the higher cut-off voltage given by the battery manufacturer. At this point, the battery is assumed to be fully charged. A fully charged battery is discharged by 5% SoC intervals until the SoC decreases to 80%. Then, the discharge interval is increased to 10% and the battery is discharged until its SoC drops to 20%. Then, the discharge interval is decreased to 5% and the

Table 2. The SoC–OCV relationship obtained by a battery SoC drop test.

SoC [%]/100 V_{oc} [V]	0	0.05	0.1	0.15
	6.5703	7.2301	7.3689	7.4079
SoC [%]/100 V_{oc} [V]	0.2	0.3	0.4	0.5
	7.4603	7.5421	7.5691	7.6404
SoC [%]/100 V_{oc} [V]	0.6	0.7	0.8	0.85
	7.7319	7.8731	8.0020	8.1301
SoC [%]/100 V_{oc} [V]	0.9	0.95	1	
	8.2202	8.3078	8.3813	

battery is fully discharged. The smaller SoC discharge interval is used at low and high SoC regions to observe the nonlinearity better. The sampling time of the battery SoC drop test is 0.01 s and the experiment is repeated five times. Finally, the average values are calculated based on the collected data. A battery SoC drop test was performed on the LiPo battery and the result is given in Table 2.

The OCV–SoC nonlinear relationship is modelled by the following nonlinear expression⁵⁰

$$V_{oc} = a \log(z) + be^{(z)^3} + c \quad (14)$$

where a , b and c are the constant coefficients, z is equal to SoC [%] divided by 100 and it is in the range of $[\delta, 1]$, where δ is an arbitrary small positive number. The SoC below δ is considered zero. The experimental data are curve-fitted to Cho et al.¹⁴ to calculate a , b and c . Conversely, a real-time estimation algorithm can be used to update the coefficients.⁵⁰

Current bias mitigation

In battery-powered systems, the current sensor output is the current measurement which is corrupted by two different types of stochastic noise²⁷

$$\tilde{I}_k = I_k + \beta_k + v_{i,k} \quad (15)$$

where \tilde{I}_k is the current measurement, and I_k is the true current, β_k is the bias noise and $v_{i,k}$ is the zero-mean white noise whose variance is r_i . β_k is a random walk and modelled as follows³⁹

$$\beta_k = \beta_{k-1} + \Delta\beta_k \quad (16)$$

where $\Delta\beta_k$ is the variation in β from sampling time $k-1$ to sampling time k .

In battery systems, the second measurable signal is \tilde{V}_t . Note that, measured \tilde{V}_t is a function of true states, including V_{oc} , I_a and true input current I . However, estimated \hat{V}_t is a function of estimated states, including \hat{V}_{oc} , \hat{I}_a and the measured current input \tilde{I} . Considering the battery states converge to their actual values, the difference between the measured \tilde{V}_t and the estimated

\hat{V}_t must be caused by the current sensor measurement error. Therefore, one sampling time step difference of $(\tilde{V}_t - \hat{V}_t)$ provides the required information to calculate β in real time. The measurement model of the terminal voltage is given by

$$\tilde{V}_{t,k} = V_{oc,k} - I_k R_0 - I_{a,k} R_p + v_{V_t,k} \quad (17)$$

Rewrite equation (17) for the previous sampling time

$$\tilde{V}_{t,k-1} = V_{oc,k-1} - I_{k-1} R_0 - I_{a,k-1} R_p + v_{V_t,k-1} \quad (18)$$

Note that $v_{V_t,k}$ is independent of $v_{V_t,k-1}$. Subtract equation (18) from equation (17)

$$\Delta \tilde{V}_{t,k} = \Delta V_{oc,k} - \Delta I_k R_0 - \Delta I_{a,k} R_p + \Delta v_{V_t,k} \quad (19)$$

where $\Delta(\cdot)_k = (\cdot)_k - (\cdot)_{k-1}$ and $\Delta v_{V_t,k} = v_{V_t,k} - v_{V_t,k-1}$. To calculate the one-step difference of the measurement residual, the estimate of ΔV_t is required. First, the estimate of $V_{t,k}$ is calculated according to the noisy current input measurement as follows

$$\hat{V}_{t,k} = \hat{V}_{oc,k} - \tilde{I}_k \hat{R}_0 - \hat{I}_{a,k} \hat{R}_p \quad (20)$$

Similarly, the estimate of V_t at sampling time $k-1$ can be written as follows

$$\hat{V}_{t,k-1} = \hat{V}_{oc,k-1} - \tilde{I}_{k-1} \hat{R}_0 - \hat{I}_{a,k-1} \hat{R}_p \quad (21)$$

Subtract equation (21) from equation (20)

$$\Delta \hat{V}_{t,k} = \Delta \hat{V}_{oc,k} - \Delta \tilde{I}_k \hat{R}_0 - \Delta \hat{I}_{a,k} \hat{R}_p \quad (22)$$

In equation (22), to calculate the difference of OCV at two sampling points, we could use the estimated SoC at two sampling points and convert them to the corresponding OCV using the SoC–OCV relationship. However, two estimated SoC could have inconsistent values to charging (increasing SoC) or discharging (decreasing SoC) of the battery. Instead, first, the previous value of SoC is calculated using the following CC equation

$$\hat{z}_{k-1} = z_k + \frac{[\tilde{I}_k - \hat{\beta}_k] \Delta t}{Q_{\max}} \quad (23)$$

where Q_{\max} is the maximum available capacity and z_k is substituted by the estimated z_k from the KF. Then, the calculated \hat{z}_{k-1} is transformed into the estimated $\hat{V}_{oc,k-1}$ through the SoC–OCV relationship. The estimated OCV difference is calculated by subtracting $\hat{V}_{oc,k-1}$ from $\hat{V}_{oc,k}$, that is, $\Delta \hat{V}_{oc,k} = \hat{V}_{oc,k} - \hat{V}_{oc,k-1}$.

The one sampling time step difference of the measurement residual can be calculated by subtracting equation (22) from equation (19) as follows

Algorithm 1 SoC estimation algorithm based on NiKF

```

1: Initialise:  $\hat{x}_0^-$ ,  $P_0^-$ ,  $\hat{\beta}_0^-$ ,  $p_{\beta,0}$ ,  $\theta_0$ 
2: while  $0 < z < 1$  do
3: Calculate the model parameter using (12) & (13)
4: Update  $\hat{\beta}_k^-$  and  $p_{\beta,k}$ 
5:  $K_{\beta,k} = p_{\beta,k} (p_{\beta,k} + r_{\beta})^{-1}$ 
6:  $\hat{\beta}_k = \hat{\beta}_k^- + K_{\beta,k} \Delta \beta_k$ 
7:  $p_{\beta,k} = (1 - K_{\beta,k}) p_{\beta,k}^-$ 
8: Calculate  $\hat{I}_k = I_k - \hat{\beta}_k$ 
9: Propagate  $\hat{\beta}_k$  and  $p_{\beta,k}$ :
10:  $\hat{\beta}_{k+1}^- = \hat{\beta}_k$ 
11:  $p_{\beta,k+1} = p_{\beta,k} + q_{\beta}$ 
12: Update  $\hat{x}_k^-$  and  $P_k^-$ 
13:  $K_k = (P_k^- C^T) (C P_k^- C^T + R + D r_{i,k} D^T)^{-1}$ 
14:  $\hat{x}_k = \hat{x}_k^- + K_k [y_k - (C \hat{x}_k^- + D \hat{I}_k)]$ 
15:  $P_k = (1 - K_k C) P_k^- (1 - K_k C)^T + K_k D r_{i,k} D^T K_k^T + K_k R K_k^T$ 
16: Propagate  $\hat{x}_k$  and  $P_k$ :
17:  $\hat{x}_{k+1}^- = A \hat{x}_k + B \hat{I}_k$ 
18:  $P_{k+1}^- = A P_k A^T + B r_{i,k} B^T + Q$ 
19: Repeat

```

$$\begin{aligned} \Delta[\Delta V_{t,k}] &= \Delta \tilde{V}_{t,k} - \Delta \hat{V}_{t,k} \\ &= \Delta V_{oc,k} - \Delta I_k R_0 - \Delta I_{a,k} R_p + \Delta v_{V_t,k} \\ &\quad - \Delta \hat{V}_{oc,k} - \Delta \tilde{I}_k \hat{R}_0 - \Delta \hat{I}_{a,k} \hat{R}_p \\ &= (\Delta V_{oc,k} - \Delta \hat{V}_{oc,k}) + (\Delta I_k - \Delta \tilde{I}_k) \hat{R}_0 \\ &\quad + (\Delta I_{a,k} - \Delta \hat{I}_{a,k}) \hat{R}_p + \Delta v_{V_t,k} \\ &= -\Delta \beta_k \hat{R}_0 - \Delta v_{i,k} \hat{R}_0 + \Delta v_{V_t,k} \end{aligned} \quad (24)$$

The difference $\Delta \beta_k$ can be calculated as follows

$$\Delta \beta_k = -\frac{\Delta[\Delta V_{t,k}]}{\hat{R}_0} + e_{s,k} \quad (25)$$

where $e_{s,k} = \Delta v_{V_t,k} / \hat{R}_0 - \Delta v_{i,k}$ is a zero-mean white noise. Directly substituting $\Delta \beta_k$ into equation (21) would amplify undesired noises in the estimated β values. Thus, the standard KF is designed for estimating β_k and provided in Algorithm 1. Details of the algorithm are presented in the next section.

SoC estimation

The SoC propagation equation is given by

$$z_{k+1} = z_k - \frac{\hat{I}_k \Delta t}{Q_{\max}} + w_{z,k} \quad (26)$$

where $w_{z,k}$ is a zero-mean Gaussian white noise. The current I_a is propagated as follows

$$I_{a,k+1} = \alpha I_{a,k} + (1 - \alpha) \hat{I}_k + w_{I_{a,k}} \quad (27)$$

where $w_{I_{a,k}}$ is a white noise with zero mean. Note that $w_{z,k}$ is independent of $w_{I_{a,k}}$. The measurement equation

is given in equation (17), where V_{oc} is a nonlinear function of z . The SoC estimation algorithm has linear state propagation equations (26) and (27) and nonlinear measurement equation (17). Consider the following generic model for a battery system

$$x_{k+1} = Ax_k + Bu_k + w_{x,k} \quad (28a)$$

$$y_k = h(x_k) + Du_k + v_{y,k} \quad (28b)$$

where $h(\cdot)$ is a nonlinear function

$$\begin{aligned} x_k &= [I_{a,k} \quad z_k]^T, y_k = \tilde{V}_{t,k}, u_k = \hat{I}_k \\ A &= \begin{bmatrix} \hat{\alpha}_k & 0 \\ 0 & 1 \end{bmatrix}, B = \begin{bmatrix} 1 - \hat{\alpha}_k \\ -\frac{\Delta t}{Q_{max}} \end{bmatrix}, w_{x,k} = \begin{bmatrix} w_{I_a,k} \\ w_{z,k} \end{bmatrix} \\ C &= \left. \frac{\partial y_k}{\partial x} \right|_{x=\hat{x}_k}, D = -\hat{R}_0, v_{y,k} = v_{V_t,k} \end{aligned} \quad (29)$$

x_k is the state vector, y_k is the measurement vector and u_k is the input. $w_{x,k}$ and $v_{y,k}$ are the process and measurement zero-mean white noises with known covariance matrices Q and R , respectively. They are independent of each other and assumed to be stationary over time.

In practice, it is expected that the standard KF's performance degrades due to the noisy input current measurement. Therefore, standard KF algorithm given in Kasdin⁵¹ is reconstructed by considering the input current measurement model given in equation (15). Note that u in equations (28a) and (28b) is replaced by \hat{I}_k in battery systems.

We are to derive the standard KF based on the generic model of the battery system. The derivation of the noisy input Kalman filter (NiKF) starts with updating the priori prediction of the state vector as follows

$$\hat{x}_k = \hat{x}_k^- + K_k(y_k - \hat{y}_k) \quad (30)$$

where $(\cdot)^-$ implies the priori prediction of (\cdot) , K_k is the Kalman gain and the $(y_k - \hat{y}_k)$ is the measurement residual. The derivation of the update part starts with defining the posterior state estimation error given as follows

$$\begin{aligned} e_k &= x_k - \hat{x}_k \\ &= x_k - \hat{x}_k^- - K_k(Cx_k + DI_k + v_{y,k} - C\hat{x}_k^- - D\hat{I}_k) \\ &= x_k - \hat{x}_k^- - K_k[Cx_k + D(\tilde{I}_k - \beta_k - v_{i,k}) \\ &\quad + v_{y,k} - C\hat{x}_k^- - D(\tilde{I}_k - \hat{\beta}_k)] \\ &= (I - K_kC)e_k^- - K_kv_{y,k} + K_kDv_{i,k} \\ &\quad + K_kD(\hat{\beta}_k - \beta_k) \end{aligned} \quad (31)$$

where $K_kD(\hat{\beta}_k - \beta_k)$ term is neglected by assuming $\lim_{t \rightarrow \infty} \hat{\beta} \rightarrow \beta$. The approximation of equation (31) is given by

$$e_k = (I - K_kC)e_k^- - K_kv_{y,k} + K_kDv_{i,k} \quad (32)$$

The posterior state estimation error covariance matrix is as follows

$$\begin{aligned} P_k &= E[e_k e_k^T] \\ &= E[((I - K_kC)e_k^- + K_kDv_{i,k} - K_kv_{y,k}) \\ &\quad ((I - K_kC)e_k^- + K_kDv_{i,k} - K_kv_{y,k})^T] \\ &= (I - K_kC)P_k^-(I - K_kC)^T \\ &\quad + K_kDr_{i,k}D^T K_k^T + K_kRK_k^T \end{aligned} \quad (33)$$

where $E[\cdot]$ represents the expectation operator and $r_{i,k}$ is the variance of $v_{i,k}$. Note that $v_{y,k}$, $v_{i,k}$ and e_k^- are independent of each other.

The Kalman gain matrix is derived by minimising the trace of P_k . The trace of P_k is the sum of the mean squared errors. Expand equation (33) as follows

$$\begin{aligned} P_k &= P_k^- - K_kCP_k^- - P_k^-C^TK_k^T \\ &\quad + K_k(CP_k^-C^T + Dr_{i,k}D^T + v_{y,k})K_k^T \end{aligned} \quad (34)$$

Taking the trace of equation (34) gives

$$\begin{aligned} \text{trace}[P_k] &= \text{trace}[P_k^-] - 2 \times \text{trace}[K_kCP_k^-] \\ &\quad + \text{trace}[K_k(CP_k^-C^T + Dr_{i,k}D^T + R)K_k^T] \end{aligned} \quad (35)$$

Differentiate equation (35) with respect to K_k

$$\begin{aligned} \frac{d\text{trace}[P_k]}{dK_k} &= -2(CP_k^-)^T \\ &\quad + 2K_k(CP_k^-C^T + Dr_{i,k}D^T + R) \end{aligned} \quad (36)$$

Equalising equation (36) to zero and solving for K_k yield

$$K_k = (P_k^-C^T)(CP_k^-C^T + R + Dr_{i,k}D^T)^{-1} \quad (37)$$

The state is propagated as follows

$$x_{k+1} = Ax_k + BI_k \quad (38)$$

The posterior error covariance matrix is propagated as follows

$$\begin{aligned} e_{k+1}^- &= x_{k+1} - \hat{x}_{k+1}^- \\ &= Ax_k + BI_k + w_{x,k} - A\hat{x}_k^- - B\hat{I}_k \\ &= Ax_k + B(\tilde{I}_k - \beta_k - v_{i,k}) + w_{x,k-1} \\ &\quad - A\hat{x}_k^- - B(\tilde{I}_k - \hat{\beta}_k) \\ &= A(x_k - \hat{x}_k^-) + w_{x,k} - Bv_{i,k} - B(\hat{\beta}_k - \beta_k) \end{aligned} \quad (39)$$

where $(\cdot)_k^-$ represents the priori prediction of $(\cdot)_k$. In equation (39), $B(\hat{\beta}_k - \beta_k)$ term is neglected since $\lim_{t \rightarrow \infty} \hat{\beta} \rightarrow \beta$ in most practical cases. The final expression of the priori state prediction error is given as follows

$$e_{k+1}^- = Ae_k + w_{x,k} - Bv_{i,k} \quad (40)$$

The prior covariance matrix is expressed as follows

$$\begin{aligned} P_{k+1}^- &= E[e_{k+1}^- e_{k+1}^{-T}] \\ &= E[(Ae_k + w_{x,k} - Bv_{i,k})(Ae_k + w_{x,k} - Bv_{i,k})^T] \\ &= AP_k A^T + Br_{i,k} B^T + Q \end{aligned} \quad (41)$$

Note that e_k , $w_{x,k}$ and $v_{i,k}$ are independent of each other. The NiKF is summarised in Algorithm 1.

Simulations and results

The first random noise corrupting the current measurement is the random walk bias β . The difference between β_k and β_{k-1} is an independent random increment which follows the Gaussian distribution. Its mean and variance are given as follows

$$E[\beta_k - \beta_{k-1}] = 0 \quad (42a)$$

$$E\{[\beta_k - \beta_{k-1}][\beta_k - \beta_{k-1}]^T\} = \sigma_\beta^2 \Delta t \quad (42b)$$

where σ_β is a positive constant. The random increment is expressed by

$$\Delta\beta_k = \eta_k \Delta t \quad (43)$$

where η_k is a random number generated from the Gaussian distribution. Equation (42a) must be satisfied, therefore

$$E[\Delta\beta_k] = E[\eta_k \Delta t] = E[\eta_k] \Delta t = 0 \quad (44)$$

The mean value of η_k must be zero, that is, $E[\eta_k] = 0$. The variance of η_k must satisfy the property of random increment given in equation (42a)

$$E[\eta_k \Delta t \eta_k^T \Delta t] = E[\eta_k \eta_k^T] (\Delta t)^2 = \sigma_\beta^2 \Delta t \quad (45)$$

Hence, the variance of η_k can be calculated by

$$E[\eta_k \eta_k^T] = \frac{\sigma_\beta^2}{\Delta t} \quad (46)$$

The second noise corrupting the current measurement is the white noise which is a typical sensor noise

whose mean is zero and distribution is Gaussian or normal

$$E[v_{i,k}] = 0 \quad (47a)$$

$$E[v_{i,k} v_{i,k}^T] = \sigma_{v_i}^2 \quad (47b)$$

It is assumed that the η_k is not correlated with the white noise $v_{i,k}$.

The simulated battery has the capacity of 0.85 Ah. It is fully discharged under two different dynamic loadings shown at the bottom of Figures 7 and 8. During the process, the bias noise and the white noise are added to the current input in every 0.01 s. The true battery model parameters are chosen similar to ones in equation³² and set to

$$[R_0 \ R_p \ C_p] = [0.3\Omega \ 0.1\Omega \ 10F] \quad (48)$$

For the simulation purposes, the initial β is randomly generated within the sample space whose lower bound is 0 and higher bound is 250 mA, σ_β is equal to 10^{-3} and the initial p_β is set to 10^{-3} . $\Delta\beta$ is calculated using equation (43). True β is then calculated in every calculation step by adding $\Delta\beta$ to the previous β .

The initial state I_a is set to 0, whereas the initial estimate z is randomly drawn from the uniform distribution in $[0,1]$. The initial priori error covariance matrix is set to $P_1^- = [10^{-3} \ 0; 0 \ 10^{-3}]$. The coefficients of the nonlinear SoC-OCV relation are as follows: $a = 0.2032$, $b = 0.3783$ and $c = 7.401$. The small-positive scalar delta is set to $\delta = 0.003$. The available voltage sensors can measure \hat{V}_i with the error of $1-2$ mV.²⁷ Therefore, we assume the $\pm 3\sigma_V = \pm 1.5$ mV, and the standard deviation in V_i , σ_V , is calculated to be $\sigma_V = 0.05$ mV. We also tested the algorithm with larger σ_V values, such as $\sigma_V = 1$ and $\sigma_V = 10$ mV. In comparison with the current bias noise, the white noise in the current measurement does not have a significant effect on the SoC estimation.²⁷ Therefore, the standard deviation in v_i , σ_{v_i} , is set to the same values as σ_V . Q is set to $[10^{-3} \ 0; 0 \ 10^{-3}]$.

Figures 3 and 4 show that the online parameter estimation algorithm successfully calculates the model parameters under two different dynamic loadings. In both cases, R_0 converges to its true value fast. However, R_p and C_p show more tiny fluctuations depending on the current input profile. This is expected because R_p and C_p define the response of the battery to the dynamic loading. However, these fluctuations do not have a significant effect on the SoC estimation error. Furthermore, C_p and R_p have the opposite reaction to keep the time constant of the battery constant. From MPI results, it can be concluded that the adaptive law-based parameter identification method can successfully estimate the model parameters under the noisy current input measurement.

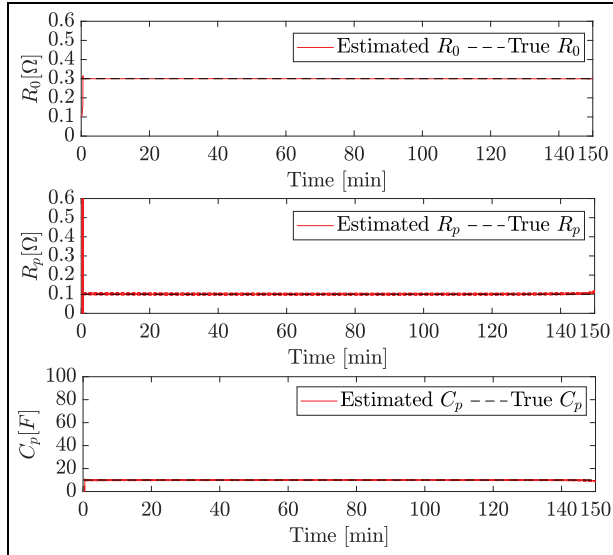


Figure 3. ECM battery parameter estimation under DST cycle.

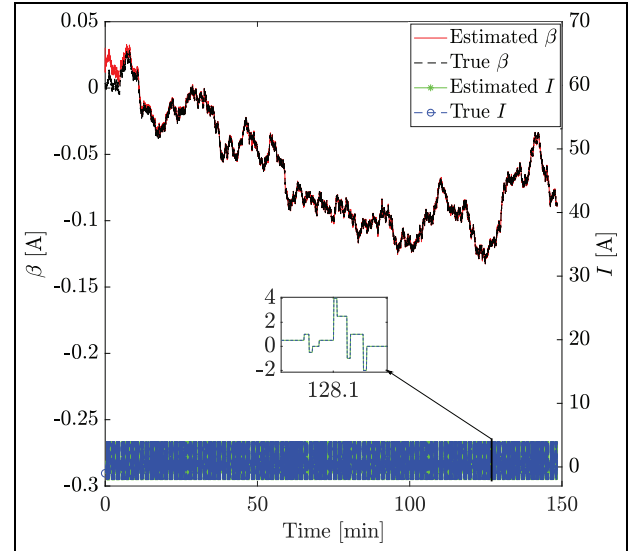


Figure 5. Bias estimation results under DST cycle.

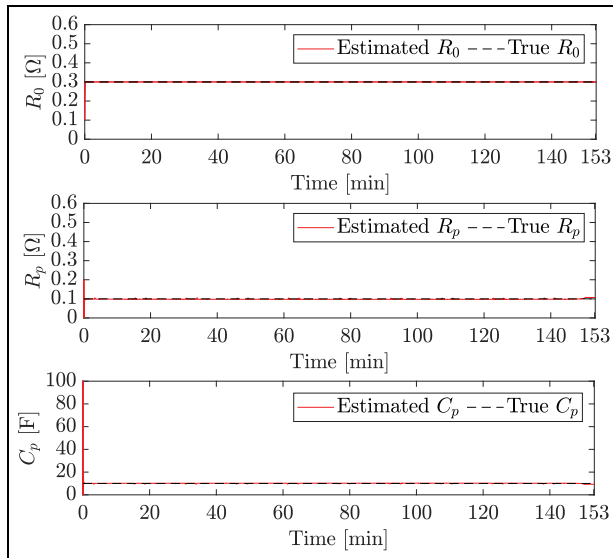


Figure 4. ECM battery parameter estimation under HPPC cycle.

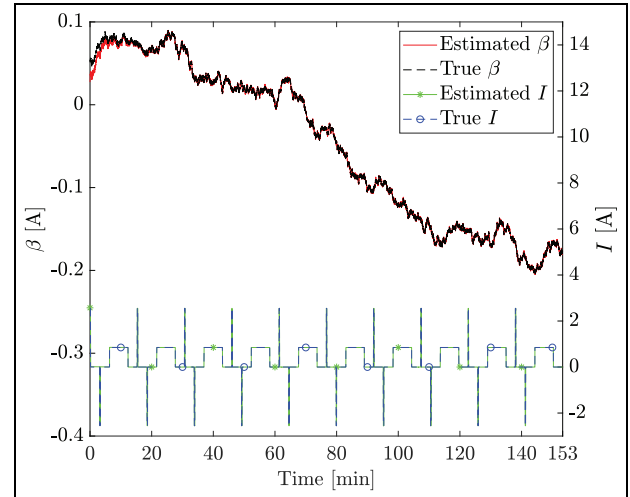


Figure 6. Bias estimation results under HPPC cycle.

Calculated parameters are then fed to the SoC estimation algorithm. The estimation of β and the current measurement are shown in Figures 5 and 6. Although the actual current bias does not change so drastically in EV applications,³¹ an extreme case is generated to test the performance of the algorithm. The maximum true bias reaches 120 mA in the dynamic stress test (DST) simulation, whereas it is around 250 mA in the HPPC test. In both scenarios, the algorithm accurately estimated β . β converges fast and minimises the effect of the initial error.

The results show that the proposed algorithm can estimate β with reasonable accuracy without depending on the current input profile. Once the estimated β is available, the bias measurement is corrected by subtracting $\hat{\beta}$ from \tilde{I} .

Figures 7 and 8 show the SoC estimation under the measured current input and the corrected current input along with the current input estimations. The mean absolute error (MAE), root mean square error (RMSE) and maximum percentage error (MAXE) of the SoC estimation are used to quantify the performance of the proposed algorithm. The MAXE in SoC estimation is reduced from around 11.3% to 0.56% under the HPPC cycle. It is decreased from 7.2% to 0.78% under the DST cycle. The battery experiment is also conducted to validate the proposed algorithm.

Figure 9 demonstrates β and SoC estimation results under different noises in terms of the standard deviation in v_V and v_i . The results show that an increase in the standard deviation in v_V and v_i increases the fluctuations in the β estimation. However, this increase does not have a significant effect on the estimated SoC values. It can be concluded that the proposed algorithm

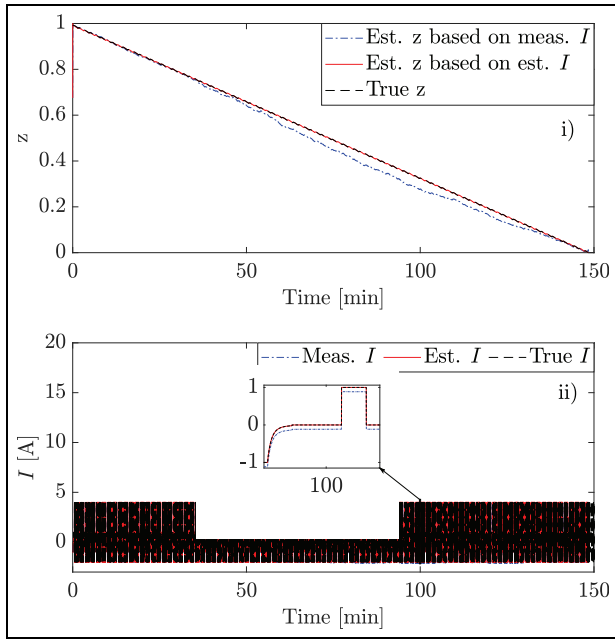


Figure 7. SoC and I estimation results under DST cycle: (i) SoC estimation results and (ii) current measurement correction result.

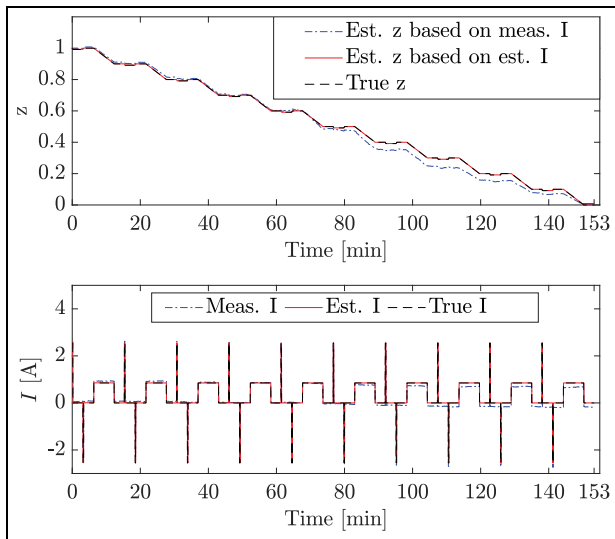


Figure 8. SoC and I estimation results under HPPC cycle: (i) SoC estimation results and (ii) current measurement correction result.

can remove the SoC error due to the current bias noise when the V_t measurement has different noise variance values.

Figure 10 shows the parameter estimation based on the battery experimental data. The parameters converge to their values fast. R_0 shows a stable value around 0.18Ω until the battery is fully discharged. In comparison with R_0 , R_p value increases dramatically at the end of the battery test. This is due to an increase in the residuals of the electrochemical reaction that takes

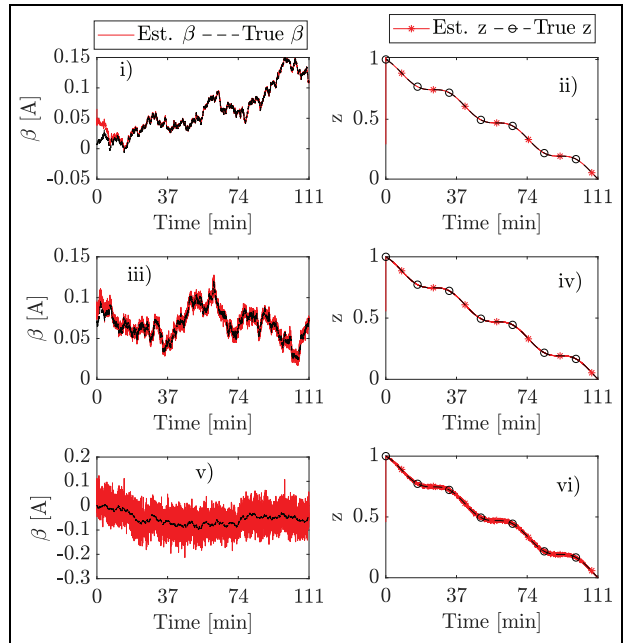


Figure 9. β and SoC estimation results with different white noise standard deviations in \hat{V}_t and \hat{I} : (i–ii) β and SoC estimation results with $\sigma_V = 0.0005$ and $\sigma_I = 0.0005$, (iii–iv) β and SoC estimation results with $\sigma_V = 0.001$ and $\sigma_I = 0.001$, (v–vi) β and SoC estimation results with $\sigma_V = 0.01$ and $\sigma_I = 0.01$.

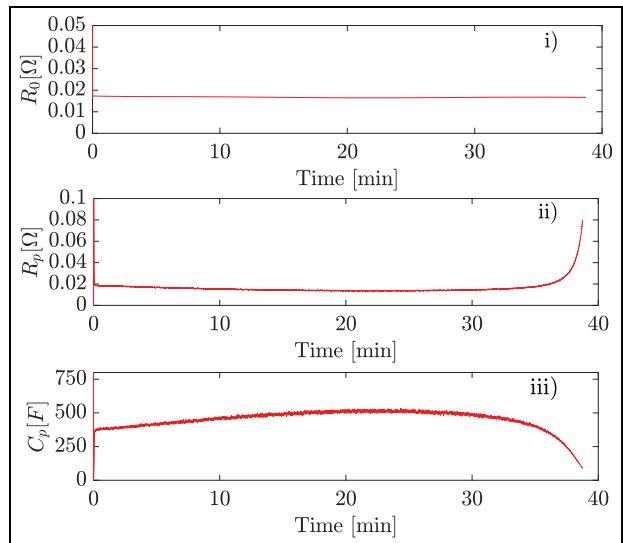


Figure 10. Parameter estimation results by experiment.

place inside the battery. C_p shows the opposite trend compared to R_p because of the battery's time constant. Figure 11 shows the SoC estimation result along with the beta estimation and corrected current measurement. The current drift is calculated at around 20 mA. However, it insignificantly changes around this magnitude due to the nonlinear relationship of the SoC–OCV curve. The current drift estimation result is similar to the one in Liu et al.³¹ The MAXE in SoC estimation is reduced from 1.74% to 1.12% in the battery

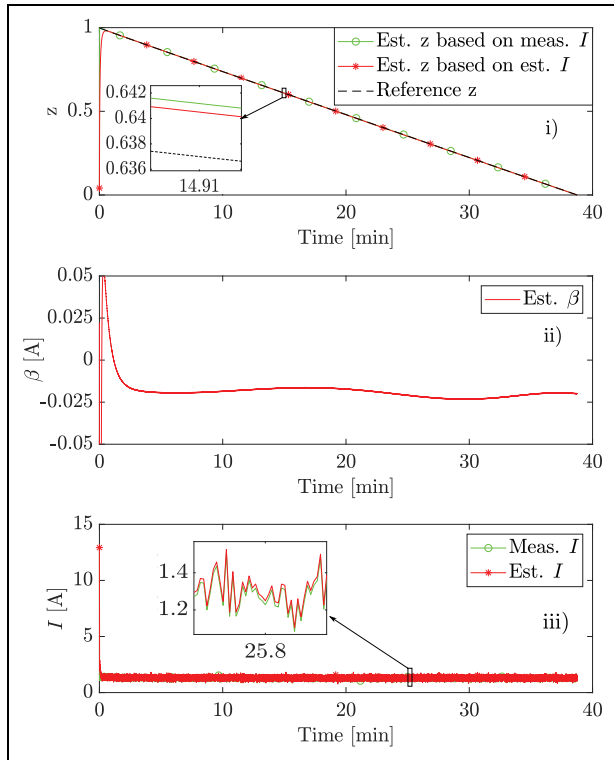


Figure 11. SoC estimation results by experiment.

experiment. Table 3 summarises MAE, RMSE and MAXE in SoC estimation for computer simulations and battery experiment. These results show that the proposed algorithm can successfully mitigate the input current measurement error. This significantly reduces the error in the SoC estimation. Results based on the experimental data validate the capability of the algorithm to adapt to real-world applications.

Conclusion and future work

The corrupted current sensor measurements, variations in the operational conditions and battery degradation are inevitable in battery-powered applications. Unlike the majority of the SoC estimation algorithms in the literature, the current measurement is corrupted by two stochastic noises in practice. This deteriorates the SoC estimation accuracy, resulting in shorter battery pack life or passenger safety risks due to overcharging/overdischarging. This study proposes an online SoC estimation algorithm that mitigates the input current measurement noise. The method significantly reduces the SoC estimation error and increases the reliability of the BMS. The battery model parameters are estimated online using an adaptive law-based parameter estimation algorithm. The input current measurement is modelled by considering the following two noises: the zero-mean white noise v_i with a known variance and the random walk bias noise β . Moreover, the standard KF is modified according to

Table 3. Summary of SoC estimation errors according to measured current and estimated current.

Error in z	With est. I	With meas. I
RMSE in DST	0.000441	0.028
RMSE in HPPC	0.000271	0.0524
RMSE in experiment	0.00374	0.00547
MAE in DST	0.0000901	0.021
MAE in HPPC	0.0000747	0.0433
MAE in experiment	0.00692	0.00947
MAXE in DST	0.78%	72%
MAXE in HPPC	0.56%	11.3%
MAXE in experiment	1.12%	1.74%

RMSE: root mean square error; DST: dynamic stress test; HPPC: hybrid pulse power characterisation; MAE: mean absolute error; MAXE: maximum percentage error.

the input current measurement model. The current input measurement is used in the state propagation and update equations. Hence, more accurate current input measurement leads to more reliable SoC estimation. The proposed algorithm accurately estimates the bias noise in the input current and corrects the input current measurement. The proposed algorithm is assessed by computer simulations and battery experiment. It is found that the proposed algorithm significantly mitigates the current measurement error source in SoC estimation and increases the SoC estimation accuracy. The current work presents an engineering practice and a theoretical framework for estimating the SoC based on noisy input current measurements. In conclusion, our work provides a more realistic understanding of the battery SoC estimation problem taking place in practice.

The future work will investigate the accuracy of β estimation based on the difference between the calculated SoC–OCV model and the true SoC–OCV model by further computational simulations and battery experiments. The further battery experiments will be conducted in terms of the longer time duration to observe a larger current bias noise. Then, the performance of the proposed algorithm will be assessed based on this experimental data.

Acknowledgement

The authors thank the Republic of Türkiye Ministry of National Education for funding support for the first author's PhD at the University of Leeds.

Authors' contributions

O.K. made a contribution in algorithm design and implementation, performed the computer simulation and battery experiment, and participated in writing original draft, review and editing. J.K. made a contribution in algorithm design, review, editing and supervision.


Declaration of conflicting interests

The author(s) declared no potential conflicts of interest with respect to the research, authorship and/or publication of this article.

Funding

The author(s) received no financial support for the research, authorship and/or publication of this article.

ORCID iD

Onur Kadem  <https://orcid.org/0000-0002-4192-1047>

Data availability

Data available on request from the authors.

References

1. Waag W, Fleischer C and Sauer DU. Critical review of the methods for monitoring of lithium-ion batteries in electric and hybrid vehicles. *J Power Sourc* 2014; 258: 321–339.
2. Li S, Zou C, Küpper M, et al. Model-based state of charge estimation algorithms under various current patterns. *Energ Proc* 2009; 158: 2806–2811.
3. Cottis RA. 4 – Electrochemical noise for corrosion monitoring. *Techniq Corros Monit* 2008; 2008: 86–110.
4. Yao Q, Lu DDC and Lei G. Rapid open-circuit voltage measurement method for lithium-ion batteries using one-cycle bipolar-current pulse. *IEEE J Emerg Select Topic Ind Electron* 2021; 2(2): 132–141.
5. Guo Y, Yang D, Zhang Y, et al. Online estimation of SOH for lithium-ion battery based on SSA-Elman neural network. *Prot Control Mod Power Syst* 2022; 7: 40.
6. Li D, Yang D, Li L, et al. Electrochemical impedance spectroscopy based on the state of health estimation for lithium-ion batteries. *Energies* 2022; 15(18): 6665.
7. Guo Y, Yang D, Zhao K, et al. State of health estimation for lithium-ion battery based on Bi-directional long short-term memory neural network and attention mechanism. *Energ Report* 2022; 8: 208–215.
8. Doyle M, Fuller TF and Newman J. Modeling of galvanostatic charge and discharge of the lithium/polymer/insertion cell. *J Electrochem Soc* 1993; 140(6): 1526–1533.
9. Newman JS and Thomas-Alyea KE. *Electrochemical systems*. 3rd ed. Hoboken, NJ: John Wiley & Sons, 2004.
10. Guo M, Sikha G and White R. Single-particle model for a lithium-ion cell: thermal behavior. *J Electrochem Soc* 2011; 158: a122.
11. Corno M, Bhatt N, Savaresi S, et al. Electrochemical model-based state of charge estimation for li-ion cells. *IEEE Trans Control Syst Tech* 2015; 23: 117–127.
12. Feng T, Yang L, Zhao X, et al. Online identification of lithium-ion battery parameters based on an improved equivalent-circuit model and its implementation on battery state-of-power prediction. *J Power Sourc* 2015; 281: 192–203.
13. Hossain M, Haque ME, Saha S, et al. State of charge estimation of li-ion batteries based on adaptive extended Kalman filter. In: *2020 IEEE power energy society general meeting (PESGM)*, Montreal, QC, Canada, 2–6 August 2020, pp. 1–5. New York: IEEE.
14. Cho IH, Lee PY and Kim JH. Analysis of the effect of the variable charging current control method on cycle life of li-ion batteries. *Energies* 2019; 2(15): 3023.
15. Shi J, Guo H and Chen D. Parameter identification method for lithium-ion batteries based on recursive least square with sliding window difference forgetting factor. *J Energ Storag* 2021; 44: 103485.
16. Kou S, Gong X, Zhu Q, et al. Parameter identification of battery model based on forgetting factor recursive least square method. In: *2018 IEEE 4th information technology and mechatronics engineering conference (ITOEC)*, Chongqing, China, 14–16 December 2018, pp. 1712–1715. New York: IEEE.
17. Xia B, Lao Z, Zhang R, et al. Online parameter identification and state of charge estimation of lithium-ion batteries based on forgetting factor recursive least squares and nonlinear Kalman filter. *Energies* 2018; 11: 10003.
18. Zhu R, Duan B, Zhang J, et al. Co-estimation of model parameters and state-of-charge for lithium-ion batteries with recursive restricted total least squares and unscented Kalman filter. *Appl Energ* 2020; 277: 115494.
19. Chaoui H, Golbon N, Hmouz I, et al. Lyapunov-based adaptive state of charge and state of health estimation for lithium-ion batteries. *IEEE Trans Ind Electron* 2015; 62(3): 1610–1618.
20. Lagraoui M, Doubabi S and Rachid A. Soc estimation of lithium-ion battery using Kalman filter and Luenberger observer: a comparative study. In: *2014 international renewable and sustainable energy conference (IRSEC)*, Ouazazate, 17–19 October 2014, pp. 636–641. New York: IEEE.
21. Xu Y, Hu M, Zhou A, et al. State of charge estimation for lithium-ion batteries based on adaptive dual Kalman filter. *Appl Math Model* 2020; 77: 1255–1272.
22. Huang C, Wang Z, Zhao Z, et al. Robustness evaluation of extended and unscented Kalman filter for battery state of charge estimation. *IEEE Access* 2018; 6: 27617–27628.
23. Ye M, Guo H, Xiong R, et al. Model-based state-of-charge estimation approach of the lithium-ion battery using an improved adaptive particle filter. *Energ Proc* 2016; 103: 394–399.
24. Zhang Z, Xia B, Li B, et al. A study on the open circuit voltage and state of charge characterization of high capacity lithium-ion battery under different temperature. *Energies* 2018; 11: 2408.
25. Lee S, Kim J, Lee J, et al. State-of-charge and capacity estimation of lithium-ion battery using a new open-circuit voltage versus state-of-charge. *J Power Sourc* 2008; 185: 1367–1373.
26. Shen P, Ouyang M, Han X, et al. Error analysis of the model-based state-of-charge observer for lithium-ion batteries. *IEEE Trans Veh Tech* 2018; 67(9): 8055–8064.
27. Zheng Y, Ouyang M, Han X, et al. Investigating the error sources of the online state of charge estimation methods for lithium-ion batteries in electric vehicles. *J Power Sourc* 2018; 377: 161–188.
28. Chen Z, Fu Y and Mi CC. State of charge estimation of lithium-ion batteries in electric drive vehicles using extended Kalman filtering. *IEEE Trans Veh Tech* 2012; 62: 1020–1030.
29. Liu D, Li L, Song Y, et al. Hybrid state of charge estimation for lithium-ion battery under dynamic operating conditions. *Int J Electr Power Energ Syst* 2019; 110: 48–61.

30. Liu Z and He H. Model-based sensor fault diagnosis of a lithium-ion battery in electric vehicles. *Energies* 2015; 8(7): 6509–6527.
31. Liu X, Chen Z, Zhang C, et al. A novel temperature-compensated model for power li-ion batteries with dual-particle filter state of charge estimation. *Appl Energ* 2014; 123: 263–272.
32. Hou J, Yang Y and Gao T. A variational Bayes based state-of-charge estimation for lithium-ion batteries without sensing current. *IEEE Access* 2012; 9: 84651–84665.
33. Chun CY, Cho B and Kim J. Implementation of discharging/charging current sensorless state-of-charge estimator reflecting cell-to-cell variations in lithium-ion series battery packs. *Int J Automot Tech* 2026; 17: 909–916.
34. Yan X, Yang Y and Guo Q. Electric vehicle battery soc estimation based on fuzzy Kalman filter. In: *2013 2nd international symposium on instrumentation and measurement, sensor network and automation (IMSNA)*, Toronto, ON, Canada, 23–24 December 2013, pp. 863–866. New York: IEEE.
35. Wang LY, Chen W, Lin F, et al. Data-driven statistical analysis and diagnosis of networked battery systems. *IEEE Trans Sustain Energ* 2017; 8(3): 1177–1186.
36. Chen H, Tian E and Wang L. State-of-charge estimation of lithium-ion batteries subject to random sensor data unavailability: a recursive filtering approach. *IEEE Trans Ind Electron* 2022; 69(5): 5175–5184.
37. Kitanidis PK. Unbiased minimum-variance linear state estimation. *Automatica* 1987; 23(6): 775–778.
38. Shu H, Zhang S, Shen B, et al. Unknown input and state estimation for linear discrete-time systems with missing measurements and correlated noises. *Int J General Syst* 2016; 45(5): 648–661.
39. Lu P, van Kampen EJ, de Visser CC, et al. Framework for state and unknown input estimation of linear time-varying systems. *Automatica* 2016; 73: 145–154.
40. Li S, Li K, Xiao E, et al. Real-time peak power prediction for zinc nickel single flow batteries. *J Power Sourc* 2020; 448: 227346.
41. Xiong R, Cao J, Yu Q, et al. Critical review on the battery state of charge estimation methods for electric vehicles. *IEEE Access* 2018; 6: 1832–1843.
42. Du J, Chen Z and Li F. Multi-objective optimization discharge method for heating lithium-ion battery at low temperatures. *IEEE Access* 2018; 6: 44036–44049.
43. Wang C, Xu M, Zhang Q, et al. Parameters identification of Thevenin model for lithium-ion batteries using self-adaptive particle swarm optimization differential evolution algorithm to estimate state of charge. *J Energ Storage* 2021; 44: 103244.
44. Zheng F, Xing Y, Jiang J, et al. Influence of different open circuit voltage tests on state of charge online estimation for lithium-ion batteries. *Appl Energ* 2016; 183: 513–525.
45. Shu X, Chen Z, Shen J, et al. State of charge estimation for lithium-ion battery based on hybrid compensation modeling and adaptive H-infinity filter. *IEEE Trans Transp Electr* 2022; 9: 945–957.
46. He H, Xiong R and Guo H. Online estimation of model parameters and state of charge of lifepo4 batteries in electric vehicles. *Appl Energ* 2012; 89(1): 413–420.
47. Chaoui H and Gualous H. Adaptive state of charge estimation of lithium-ion batteries with parameter and thermal uncertainties. *IEEE Trans Control Syst Tech* 2017; 25(2): 752–759.
48. Ioannou P and Fidan B. *Adaptive control tutorial, society for industrial and applied mathematics*. Philadelphia, PA: SIAM.
49. Afshari HH, Attari M, Ahmed R, et al. Reliable state of charge and state of health estimation using the smooth variable structure filter. *Control Eng Practice* 2018; 77: 1–14.
50. Kadem O and Kim J. Real-time state of charge-open circuit voltage curve construction for battery state of charge estimation. *IEEE Trans Veh Tech*. Epub ahead of print 13 February 2023. DOI: 10.1109/TVT.2023.3244623.
51. Kasdin NJ. *Optimal estimation of dynamical systems*, John L. Crassidis and John L. Junkins, Chapman & Hall/CRC, London, Boca Raton, 2004, ISBN 1-58488-391-X. *Int J Robust Nonlin Control* 2006; 16(7): 369–371.
52. Jarraya I, Masmoudi F, Chabchoub MH, et al. An online state of charge estimation for lithium-ion and supercapacitor in hybrid electric drive vehicle. *J Energ Storage* 2019; 26:0946.